Published by
NIGERIAN SOCIETY OF PHYSICAL SCIENCES
Available online @ https://journal.nsps.org.ng/index.php/jnsps

J. Nig. Soc. Phys. Sci. 5 (2023) 951

Journal of the Nigerian Society of Physical Sciences

Safranin O dye removal using Senna fistula activated biomass: Kinetic, equilibrium and thermodynamic studies

C. J. Ajaelu*, O. Oyedele, A. A. Ikotun, E. O. Faboro

Industrial Chemistry Programme, College of Agriculture, Engineering and Science, Bowen University, Iwo, Nigeria

Abstract

The availability of potable water has decreased in recent times due to the extensive discharge of effluents from some industries. This contaminated water poses a great danger to both human and aquatic life. *Senna fistula* was activated using phosphoric acid, H_3PO_4 and its ability to remove Safranin O from aqueous solution was investigated. The characterization of *Senna fistula* activated carbon was done by Scanning Electron Microscopy and Fourier Transform Infrared Spectroscopy. The impacts of pH, initial dye concentration, contact time, and effect of temperature were investigated. Results showed that the optimum pH for the removal of Safranin O was 4.4. The adsorption capacity increased as the initial dye concentration increased from 30 - 130 mg/L. The dye adsorption equilibrium data were properly fitted to both Freundlich and Langmuir isotherms. The maximum uptake capacity for Safranin O was 22.1 mg/g. The kinetic studies indicated rapid sorption dynamics via a second-order kinetic model. The thermodynamic parameter shows that the sorption of Safranin O on *Senna fistula* activated carbon was feasible, spontaneous and endothermic. *Senna fistula*-activated carbon was found to be cheap and efficient adsorbents for the removal of Safranin O dye from aqueous solutions.

DOI:10.46481/jnsps.2022.951

Keywords: *Senna fistula*, Safranin O, adsorbent, kinetics, thermodynamics

Article History :
Received: 20 July 2022
Received in revised form: 21 August 2022
Accepted for publication: 07 November 2022
Published: 22 December 2022

Communicated by: N. A. A. Babarinde

1. Introduction

The surge in deleterious dye wastewater emanating from industries is of alarming public health and environmental safety concerns. Around 700,000 tons of dye are produced worldwide each year, which results in 100,000 dyes being sold in the market [1, 2]. Concerns have been raised by the United Nations over the fact that more than 80 % of the world's wastewater, including more than 95 % in some of the world's poorest countries, is released into the environment without first being treated [3].

Highly polluted effluents are produced because of the considerable amount of water employed in the dyeing processes [1]. It has been observed that between 10 and 15 % of dyes meant for fibers could not adhere to them and are ultimately found as industrial effluents. These dyes infiltrate water bodies, causing colouration, a reduction in photosynthesis and dissolved oxygen, and suppression of aquatic plant growth. Carcinogenesis, mutagenesis, teratogenicity, chromosomal fractures, kidney, liver and reproductive system dysfunctions,

*Corresponding author tel. no: +2348034994404.
Email address: ajaelujohn46@gmail.com (C. J. Ajaelu)

watery eyes, itching, and asthma symptoms are all effects of water pollution in humans [4, 5].

Safranin O is a basic dye commonly referred to as basic red 2. Safranins are symmetrical 3,7-Diamino2,8-dimethyl-5-phenylphenazin-5-ium chloride's azonium compounds. Basic dyes are the most vibrant type of soluble dyes used in the textile industry to color acrylic, nylon, silk, and wood. They have a high tinctorial value; as low as 1 ppm of dye generates noticeable colour. Due to its disposal in water bodies, it poses a threat [6]. Safranin O dye causes skin irritation, eye irritation, is carcinogenic and can impact blood factors such as coagulation, induced somnolence, respiratory issues and significant alimentary tract irritations.

In order to address this global challenge of dye pollution, different dye removal techniques have been adopted by researchers. These include photocatalysis, ion exchange, electrochemical, and oxidation-reduction. These methods have high operational costs and are time-consuming. Most of these methods have deficiencies such as the high energy and reagent requirements, the low selectivity and the difficulty in removing the secondary waste generated [3].

A cheaper and more efficient technique for dye removal is adsorption. Despite the fact that adsorption is a cheaper method than other methods earlier mentioned, the cost-effectiveness of the adsorption method also depends on the ease of availability of the adsorbent. Some adsorbents are waste materials while others are purchased. The use of agricultural waste material (biosorbent) is the cheapest form of adsorbent, for it has zero cost to acquire. Some of the biosorbents used to remove dyes include coconut husk [7] African Border Tree [8], oil palm fruit [9, 10], watermelon rinds [11], okra [12], maize stuck, teak leaf [13], sugarcane bargass [14].

Senna fistula, also known as the Golden shower tree, produces pods as its ripe fruits. *Senna fistula* is a medium-sized tree native to the Indian subcontinent and also found in the southern region of Nigeria. It is frequently grown as an ornamental plant. Ripe pods are long, virtually straight, cylindrical, dark chocolate-brown fruits with a length of 45 to 60 cm and a thickness of 20-25 mm. The surface seems smooth and shiny to the human eye but is characterized by minute transverse striations under a microscope. This study is targeted at converting *Senna fistula* pod into activated carbon and investigating the removal of Safranin O dye from aqueous solutions. Contact time, temperature, adsorbent dosage, and initial Safranin O concentration were all evaluated as operational parameters.

Different isotherm and kinetic models were used to evaluate the experimental data. Thermodynamic parameters that govern the adsorption process were also investigated.

2. Materials and methods

2.1. Raw materials/chemicals

Safranin O was obtained from KEM LIGHT Laboratories PVT. Ltd, India. The structure and the physical characteristics of Safranin O are presented in Figure 1 and Table 1, respectively. NaOH (99.0 %) was obtained from Merck, Germany, NaCl (99.5 - 100 %) from Merck, Germany, and HCl (35.4 %) from BDH. The chemicals were of analytical quality. Therefore, further purifications were not carried out on them.

2.2. Preparation of Adsorbate

The adsorbate was prepared by dissolving 1 g of the Safranin O dye ($C_{20}H_{19}N_4Cl$, molecular weight 350.8 g/mol) in little quantity of distilled water in a 1 L volumetric flask. It was properly dissolved and made up to the mark with distilled water. Serial dilutions were carried out to prepare various concentrations needed for the adsorption studies.

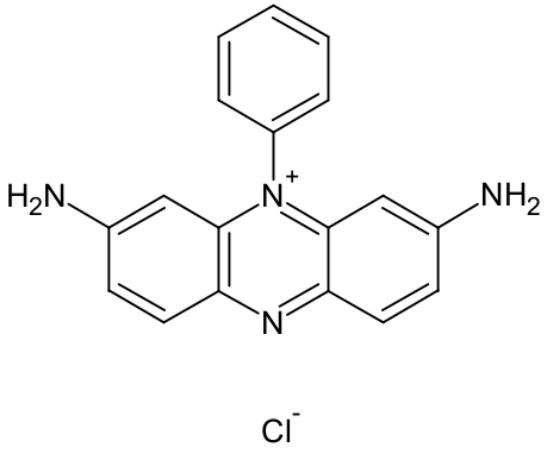

Figure 1: The molecular structure of Safranin O

Table 1: Physical characteristics of Safranin O

IUPAC Name/ Molecular formula	3,7-Diamino-2,8-dimethyl-5-phenylphenazin-5-ium chloride/ $C_{20}H_{19}ClN_4$
Common name	Safranin O, Basic red 2
CAS Number	477 - 73 - 6
Molar mass	350.85 g/mol
Appearance	Dark red
Storage Temperature	Room temperature
ε_{max}	1250-1650 at 530-534 nm in 50 % ethanol
Solubility in water	Water, 1 mg/mL, clear, dark red, red purple

2.3. Adsorbent preparation

The pods were washed properly and then oven- dried after which the pods were split and the inside were cleaned thoroughly to get rid of unwanted materials like the seeds. As a result of drying, the pods became very hard and had to be crushed to achieve smaller particle size conducive for grinding after which the crushed pods were then ground to powder. The resultant powder was passed through a sieve of mesh size 1.0 mm after which it was stored in a plastic bag for the next stage of the process.

50 g of the powdered adsorbent was measured and gently stirred into a solution of 1.0 M phosphoric acid (H_3PO_4) and kept for a day in a cool dry place. This was to give the adsorbent ample time to soak up the acid. The mixture was rinsed with distilled water and dried in an oven at 105 °C. It was then transferred into crucibles and carbonized in a Muffle furnace at 350 °C in the absence of air for 45 minutes. The carbonized sample was cooled in a desiccator and then rinsed with distilled water to remove ash. It was further washed to ensure a near-neutral pH of 6.89. It was dried in an oven at 105 °C until a constant weight was achieved after which the modified *Senna fistula* pods activated carbon MSF was stored in a glass bottle.

2.4. Adsorption studies

In this experiment, the adsorbate was Safranin O dye. For the stock solution, 1 g of Safranin O was dissolved with distilled water in a 1 L volumetric flask and made up to mark. Lower concentrations were made by repeated dilution from the stock solution. The effectiveness of MSF in removing Safranin O was measured using four different operating parameters, including pH, initial SO concentration, contact time, and solution temperature. In this study, 0.1 g of MSF was agitated with 20 ml of varying concentrations (30, 50, 70 and 90 mg/L) of SO solutions and agitated at 200 rpm in an electric shaker. A UV spectrophotometer (Shimadzu 1800 double beam) at 520 nm was used to measure the absorbance of aliquot samples at regular intervals. Equation (1) was used to calculate % removal and adsorption capacity.

$$\text{Percentage uptake capacity} = \frac{C_o - C_e}{C_o} \times 100 \tag{1}$$

$$q_e = \frac{(C_o - C_e)\,V}{w} \tag{2}$$

where q_e (mg/g) is the amount SO adsorbed, C_o (mgL^{-1}) and C_e (mgL^{-1}) are the initial and final concentrations of SO respectively. V(L) and w(g) represent the volume of SO and the weight of *Senna fistula*, respectively.

2.5. Characterization of Senna fistula

A scanning electron microscope (Zeiss Auriga HRSEM) was used to characterize the surface structure of MSF. As a thin beam of electrons scans the surface of the adsorbent in a rectangular raster, SEM measures the intensity of numerous signals created by interactions between the beam electrons and the adsorbent. In order to get a magnified image of the adsorbent, the surface property, components, and scenery of the adsorbent are determined from the signals provided by SEM [15].

Senna fistula spectra were recorded using an Agilent Technologies Cary 630 Fourier transform infrared (FTIR) spectrometer. Between 4000 and 600 cm^{-1}, spectroscopic measurements were taken. Spectroscopic analysis was used to analyze the surface chemistry of *Senna fistula* powder before and after copper adsorption. Before and after copper adsorption, the FTIR spectra indicated the functional group(s) on the *Senna fistula* surfaces.

3. Results and Discussions

3.1. Characterization

Senna fistula morphology was determined using a scanning electron microscope as shown in Figure 2. The phosphate-modified *Senna fistula* shows a rough, irregular, heterogeneous honeycomb-like surface structure with several pores and cavities which is due to the phosphate modification. The adsorption of SO resulted in less number of pores on the absorbent surface since quite a number of the pores have been occupied by the dye.

The FTIR spectra of phosphate-modified *Senna fistula* with Safranin O (MSF-SO) and the phosphate-modified *Senna fistula* (MSF) without Safranin O were compared in Figure 3 and Table 2 to identify functional groups through characteristic vibrational frequencies. Phosphate-modified *Senna fistula* with SO showed a broad and medium band around 3327 cm^{-1}, which is owing to an (OH) vibration band of a hydrogen bond due to the phosphoric acid, which is absent in MSF. The (CH) vibrational bands are responsible for the crisp and strong bands that occur at 2982 cm^{-1} to 2881 cm^{-1}. After SO adsorption, these bands remained nearly constant at 2922 cm^{-1} and 2853 cm^{-1}. (C=O) stretching vibration band coming from the carboxylic acid is responsible for the crisp and medium band at 1702 cm^{-1}. After SO dye adsorption, this band has shifted to a higher frequency of 1744 cm^{-1} and also appeared as a strong band. This denotes the chemical interaction of the oxygen atom of the C=O bond thereby forming new bonds during adsorption [16]. There is a C=N vibrational band appearing as a sharp medium band at 1593 cm^{-1} before SO adsorption. This band has almost remained unchanged at 1595 cm^{-1} after SO adsorption, thus signifying no chemical interaction of the nitrogen from the CN group [17, 18]. The (C=C) stretching vibrations are responsible for the emergence of a new sharp and medium band at 1685 cm^{-1} in MSF with SO dye but absent in MSF without SO. The P-O-C- stretching vibration is responsible for the bands at 1112.6 cm^{-1} and 980.6 cm^{-1}. After SO adsorption, these bands changed to higher frequencies of 1157 cm^{-1} and 1057 cm^{-1}, respectively.

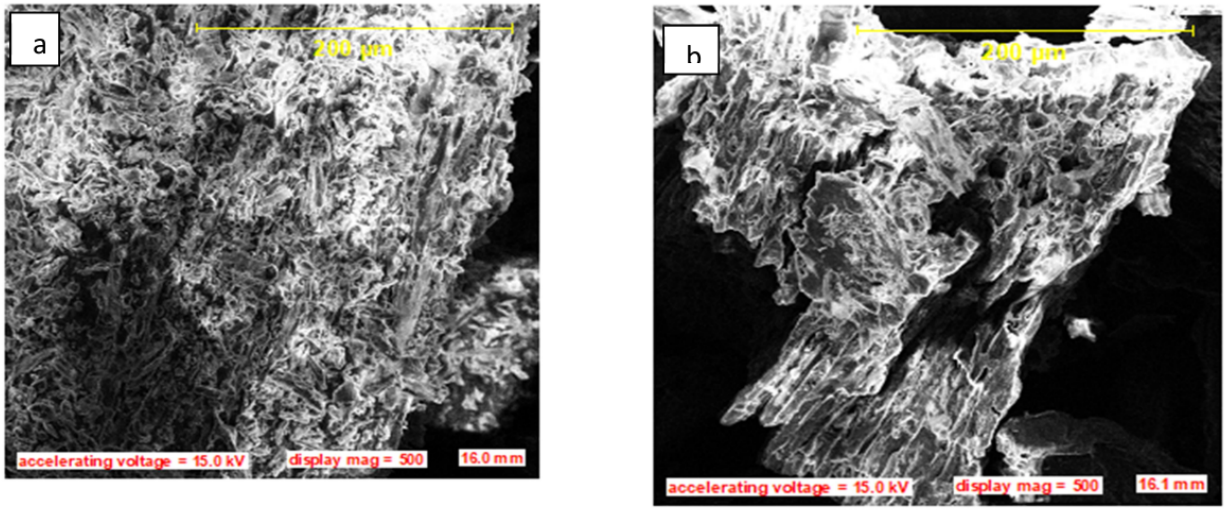

Figure 2: Typical SEM of modified *Senna fistula* (a) without and (b) with Safranin O.

Table 2: Infrared Spectral Data of MSF pre- and post- sorption of SO dye

Adsorbent	v(OH) (cm^{-1})	v(CH) (cm^{-1})	v(C=O) (cm^{-1})	v(C=N) (cm^{-1})	v(C=C) (cm^{-1})	v(C−O) (cm^{-1})	v(P-O-C) (cm^{-1})
Modified *Senna fistula* (MSF)		2982 b,m 2881 b,m	1702 m	1593 m		1165s 1034s	1113s 980s
Modified *Senna fistula* (MSF) after SO adsorption	3326.6s	1744 s 2853 s	1744 s	1595 m	1685 m	1157s 1027m	1157s 1057m

3.2. *Effect of pH*

The role played by pH in the adsorption of dye molecules is quite revealing. The pH regulates the competition between the dye molecules and hydrogen ions on the active sites of the sorbent surface [19]. The pH of the solution affects the adsorbent's surface charge and the ionization of the adsorbate [20]. Additionally, the effectiveness of adsorption in aqueous solutions is influenced by hydrogen bonds, $\pi - \pi$ interaction, and $n - \pi$ interaction [21, 22, 23]. Figure 4 demonstrates that when pH rises from 1 to 4, Safranin O adsorption capacity increases significantly. This is due to the availability of a large active site. At lower pH 1, there is competition for the available site between the hydrogen ion and the positive charge dye molecule. This leads to lower adsorption. As the pH rises, the competition between the two cations reduces, and more sites are made available for the dye molecule to adsorb on the surface of MSF. At pH greater than 4 the adsorption reaches equilibrium.

3.3. *Initial dye concentration*

The initial dye concentration has a significant influence on the adsorption capacity of the adsorbent. Figure 5 shows that the adsorption capacity increases as the initial Safranin O concentration increases from 30 -130 mg/L. This increase is due to a large number of available adsorption sites [24, 25]. In addition, the mass transfer rate of Safranin O from the bulk solution to the adsorbent surface is high. The interaction between SO and the adsorbent, MSF, is also improved by increasing the initial dye concentration. Thus, increasing the initial concentration of SO improves its adsorption. This demonstrates that the relationship between the adsorption capacity and the starting SO concentration is linear. A similar increase was reported by Rassaq et al. 2021 [26].

3.4. *Effect of Contact time*

The time required for equilibrium to be attained is very vital as it determines the effectiveness of the adsorption process as well as the cost of the wastewater treatment. The effect of contact time on the adsorption of safranin O dye is reflected in Figure 6. The Figure demonstrates that for a dye concentration of 30 mg/L, a sharp increase in contact time for the first 10 minutes significantly improved SO's adsorption ability, connoting that SO's initial rate of adsorption by the MSF was very fast. This is due to the functional adsorbent's enormous number of accessible sites, which is responsible for the increased adsorption. In addition, there was an increase in the collision rate of dye molecules. There was a gradual increase from 10 - 25 min after which equilibrium was reached. This was a result of a drastic reduction in the number of available active sites as well as a low rate of collision of dye molecules.

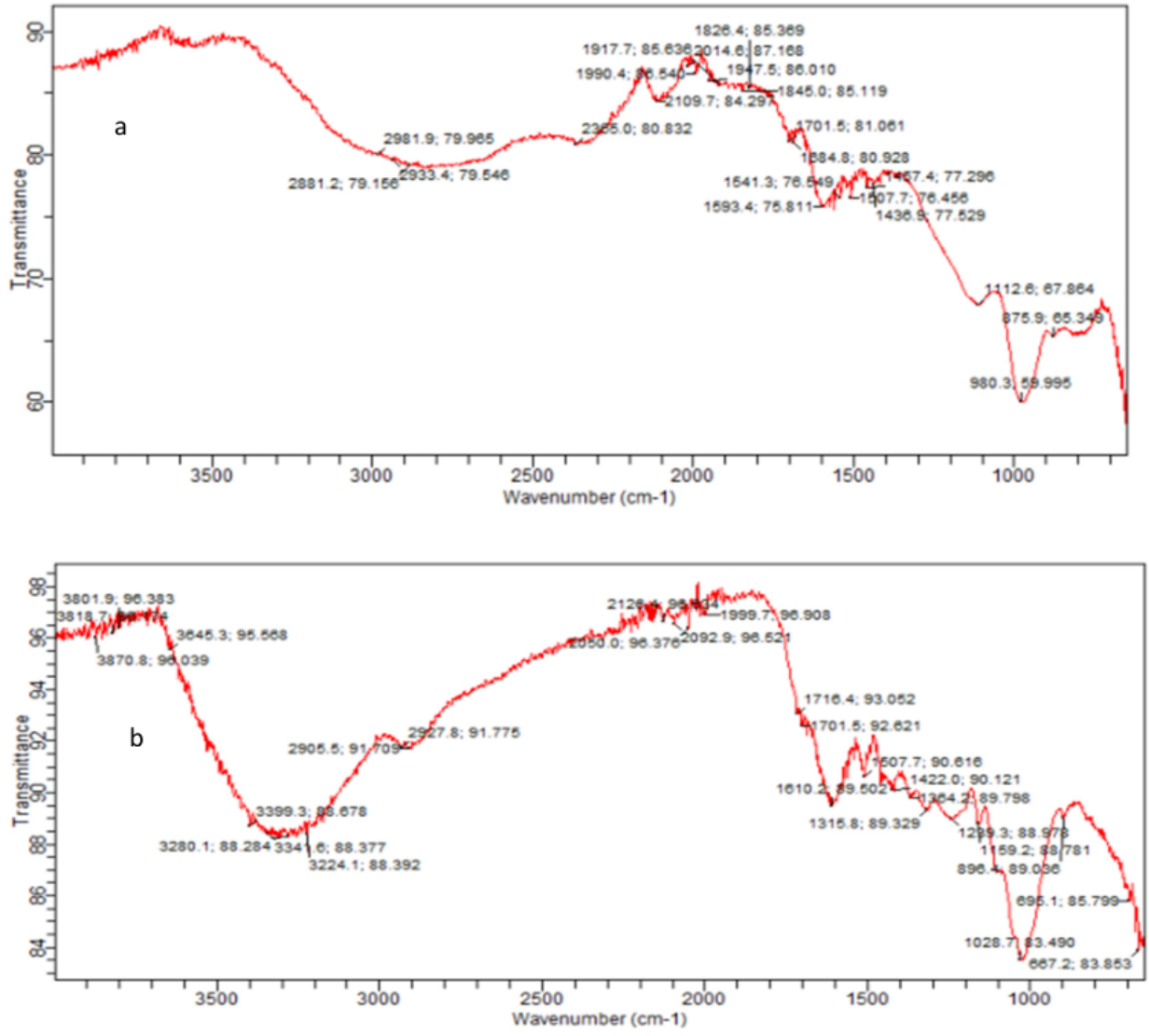

Figure 3: The FTIR of modified *Senna fistula* (a) without and (b) with Safranin O.

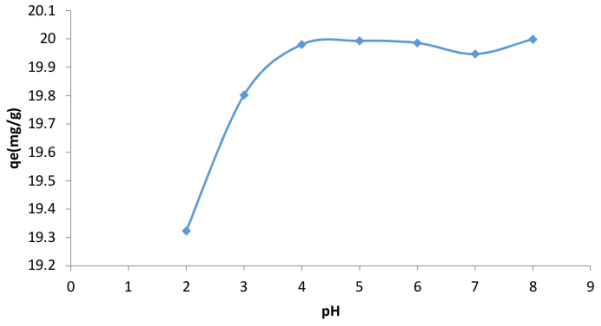

Figure 4: pH effect on the sorption of Safranin O on modified *Senna fistula*.

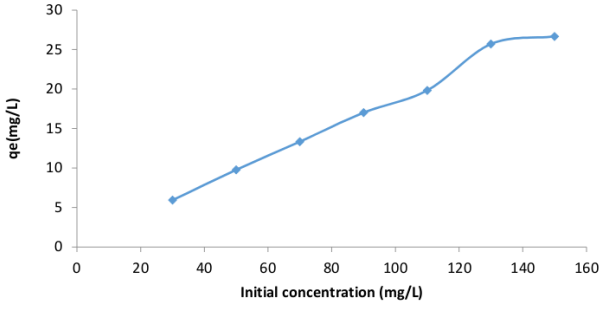

Figure 5: Initial dye effect on the sorption of Safranin O on modified *Senna fistula*

3.5. Adsorption kinetics

Studying the kinetics of the adsorption process can help in comprehending the mechanism and phases involved in the trapping of adsorbate molecules onto the adsorbent. To learn more about the sorption mechanism, two kinetic models, pseudo-first and pseudo-second order, were fitted to the experimental data.

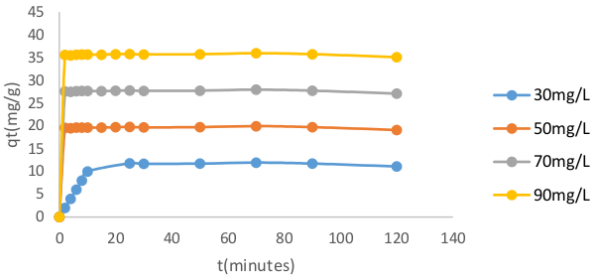

Figure 6: Contact time effect on the sorption of Safranin O on modified *Senna fistula*.

The Lagergren pseudo- first-order kinetic equation is given by

$$\log(q_e - q_t) = \log q_e - \frac{k_1 t}{2.303}, \tag{3}$$

where k_1 is a pseudo-first-order reaction's rate constant, and q_t is the amount of dye adsorbed per unit of adsorbent (mg g^{-1}) at time t (h^{-1}). The adsorption rate constant (k_1) was calculated using the $\log(q_e - q_t)$ plot against time as presented in Figure 7a.

The pseudo-second-order kinetic was introduced by Ho and McKay [27] as:

$$\frac{t}{q_t} = \frac{1}{k_2 q_e^2} + \frac{1}{q_e} t, \tag{4}$$

where k_2 (g mg^{-1} h^{-1}) is the pseudo-second-order rate constant. A linear plot of t/q_t vs t yields the q_e and k_2 as reflected in Figure 7b.

The pseudo-second-order kinetic model is the one that best fits the experimental data since its correlation factor is close to 1 and its calculated adsorption capacity is of close proximity to the experimental adsorption capacity as presented in Table 3.

3.6. Effect of Temperature

Temperature is another significant factor that directly impacts the adsorption of dyes and has an impact on the solid-solute interface and the mobility of the pollutants during adsorption. In this study, adsorption capacity increases with an increase in temperature from 308 to 318 K (Figure 8). The increase was relatively sharp from 303 - 318 K and then reached equilibrium by leveling off from 318 - 338 K. The increase in temperature increases the dye mobility in the solution and consequently increases the probability of interaction between the adsorbate and adsorbent. This investigation shows that SO adsorption is an endothermic process and favours high temperatures.

3.7. Adsorption isotherm

Isotherm study gives details about the concentration of SO adsorbed on MSF surface by correlation of experimental data to three equilibrium models namely Langmuir (Figure 9), Freundlich (Figure 10) and Temkin (Figure 11).

3.7.1. Langmuir isotherm

According to the Langmuir isotherm model, monolayer sorption occurs on a homogenous surface where there is no interaction between the molecules that are adsorbed. The model also assumes homogeneous energies for adsorption onto the surface [28, 29, 30]. The general and linear Langmuir equations are represented by equation (5) and (6), respectively.

$$q_e = \frac{X_0 b C_e}{1 + bC_e} \tag{5}$$

$$\frac{C_e}{q_e} = \frac{1}{X_0 b} + \frac{1}{X_0} C_e. \tag{6}$$

The dimensionless separation factor is given by:

$$R_L = \frac{1}{1 + bC_0} \tag{7}$$

X_0 s the maximum uptake capacity in mg/g while b is Langmuir constant. Table 4 shows that the maximum uptake capacity is 22.1 mg/g while the dimensionless separation factor is much less than 1 indicating that the adsorption of SO unto MSF is feasible and favorable.

3.7.2. Freundlich isotherm

The Freundlich isotherm is a nonlinear sorption model that describes multilayer adsorption with a heterogeneous energy distribution of active sites and interactions between adsorbed molecules [31]. The non-linear and the linear equations are presented in equations (8) and (9), respectively.

$$q_e = K_F C_e^{\frac{1}{n}} \tag{8}$$

$$\log q_e = \log K_F + \tfrac{1}{n} \log C_e, \tag{9}$$

where K_F and n are Freundlich constants related to adsorption capacity and adsorption intensity, respectively. Figure 10 presents the graph of $\log q_e$ against $\log C_e$. The n value is greater than 1 which indicates that the physical adsorption process is feasible and favourable.

3.7.3. Temkin model

Temkin's isotherm model presupposes a linear decrease in all molecules' heat of adsorption with increasing adsorbent surface coverage. Temkin's model general and linear forms are presented in equations (10) and (11), respectively.

$$q_e = \frac{RT}{\sigma} \ln \omega C_e \tag{10}$$

$$q_e = \beta \ln \omega + \beta \ln C_e, \tag{11}$$

where

$$\beta = \frac{RT}{\sigma}. \tag{12}$$

$\sigma\left(Jmol^{-1}\right)$ is the Temkin binding constant which is correlated with the heat of adsorptions, ω is the equilibrium binding constant (Lmg^{-1}), T is thermodynamic temperature and R

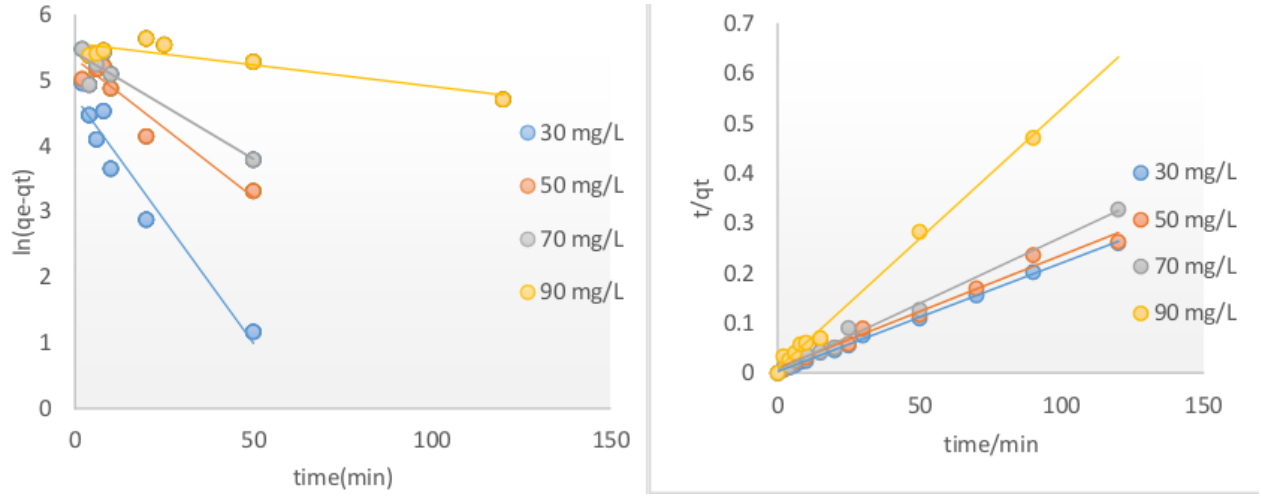

Figure 7: Kinetic plots showing (a) Pseudo-first and (b) pseudo-second order for copper adsorption onto modified *Senna fistula*.

Table 3: Kinetic adsorption parameters for the adsorption of SO on MSF

	First order kinetics				Second order kinetics		
Conc (mg/L)	q_e (calc)	q_e (exp)	k_1	R^2	q_e (calc)	k_2	R^2
30	1.03	10.8	0.0016	0.9404	11.4	0.182	0.9984
50	1.2	18.2	0.0007	0.9143	19.4	0.186	0.9995
70	1.39	25.5	0.0004	0.8907	27.4	0.187	0.9997
90	1.36	32.9	0.0121	0.8011	35.3	0.188	0.9998

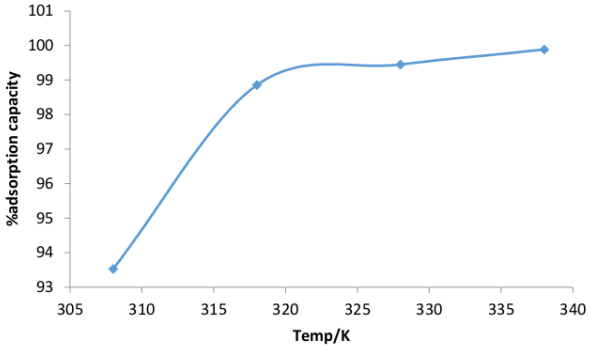

Figure 8: Effect of temperature on the adsorption of Safranin O on modified *Senna fistula*.

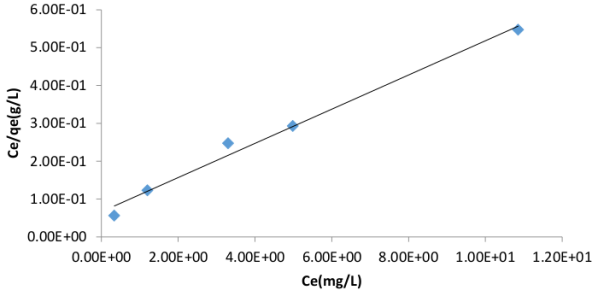

Figure 9: Langmuir isotherms for the adsorption of Safranin O onto *Senna fistula*

Table 4: Langmuir, Freundlich and Temkin Isotherms for the adsorption of Safranin O on *Senna fistula*

Langmuir	Freundlich	Temkin
X_0 = 22.1 mg/g	K_F = 1.69	σ = 13657.1
c = 0.677	n = 1.33	ω = 9141.1
R_L = 0.047	R^2 = 0.99	R^2 = 0.92
R^2 = 0.987		

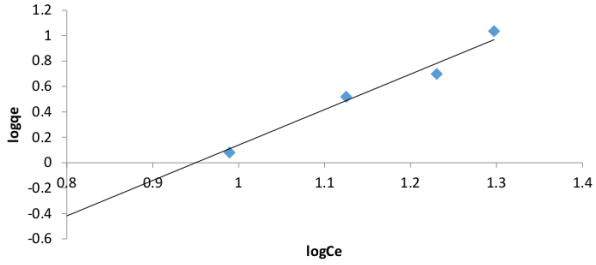

Figure 10: Freundlich isotherm for the adsorption of SO on modified *Senna fistula*

is molar gas constant (0.008314 kJ mol^{-1} K^{-1}). The Temkin correlation factor (Figure 11, Table 4) is low compared to other adsorption isotherms, hence it is not the most appropriate for explaining the adsorption process. Adsorption equilibrium isotherm demonstrates that both the Freundlich and Langmuir isotherms are the most suitable for describing the adsorption process.

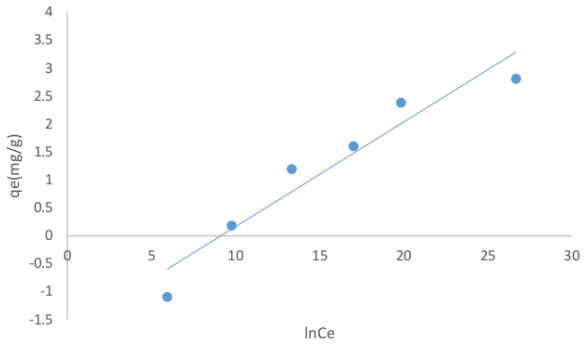

Figure 11: Temkin isotherm for the adsorption of SO on modified *Senna fistula*

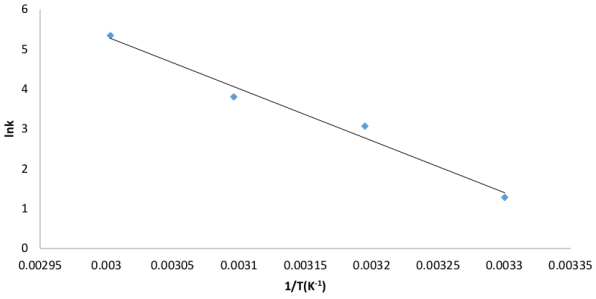

Figure 12: Thermodynamic effect of the adsorption of dye on MSF

3.8. Thermodynamics

Thermodynamic parameters such as the entropy change ΔS, enthalpy change ΔH and the free energy ΔG change were determined at different temperatures (303, 308, 313 and 318 K) using the following equations:

$$\Delta G = -RT \ln K \tag{13}$$

$$\ln K = -\frac{\Delta G}{RT} = \frac{\Delta S}{R} - \frac{\Delta H}{RT} \tag{14}$$

$$\ln k_2 = \ln A - \frac{E_a}{RT} \tag{15}$$

k_2 is the rate constant for a second-order adsorption kinetic (g/mgh), A is the Arrhenius factor, E_a is the activation energy (kJ/mol) that must be overcome for adsorption to take place, R is the gas constant (J/molK), T is the thermodynamic temperature (K).

The calculated values of ΔS, ΔH and ΔG are vital thermodynamic parameters in the adsorption process. The intercept and slope of the Van't Hoff plot of $\ln k$ against $1/T$, as shown in Figure 12, yielded the values of ΔS, ΔH, which were consistent

Table 5: Thermodynamic parameters for the adsorption of SO on modified *Senna fistula*

Adsorbent	ΔH(kJ/mol)	ΔS (J/mol)	ΔG (kJ/mol)				E_a (J/mol)
			303 K	308 K	313 K	323 K	
MSF	108.5	369.6	-5.37	-9.06	-12.7	-16.5	28.3

Table 6: Comparisons of the adsorption capacities of diverse adsorbents used for SO removal

Adsorbent	dye	Maximum adsorption capacity (mg/g)	Reference
Nano iron oxide	SO	1.91	[36]
Mango seed integument	SO	34.5	[37]
Kaolinite clay	SO	16.2	[38]
Soybean hull	SO	23.8	[39]
Senna fistula-activated carbon	SO	22.1	This study

with our previous research on Safranin O dye adsorption employing the African Border tree [8]. Table 5 presents the thermodynamic parameters for the adsorption of SO on modified *Senna fistula*. The entropy change (ΔS = 369.6 J/mol) is positive which implies the affinity of MSF for the SO dye as well as enhanced randomness at the solid-solution interface during the adsorption of SO dye onto the surface of the active sites of MSF. This results in higher uptake of SO on MSF. The enthalpy change is positive (ΔH = 108.5 kJ/mol), which is endothermic, which indicates that heat is absorbed during the adsorption process. The free energy change values ΔG = −5.37, -9.06, -12.7, and -16.5 kJ/mol at 303, 308, 313, and 318, respectively are negative which connotes the spontaneity and the feasibility of the adsorption of SO on MSF. Moreover, ΔG became more negative as temperature increased, indicating that higher temperatures actively support the feasibility and spontaneity of the adsorption process. These observations are incongruent with other findings described in several studies [7, 15, 35]. The energy of activation Ea, was determined using equation (15). The value of E_a (0.0283kJ/mol) reveals that adsorption is a physical process [32, 33, 34, 35]. The adsorption capacities of various adsorbent for Safranin O is presented in Table 6.

4. Conclusion

In this study we determined the effectiveness of phosphate modified *Senna fistula* in the adsorption of Safranin O dye from aqueous solution. The adsorbent was prepared and applied for the adsorption of Safranin O dye from aqueous solution as a function of pH, initial dye concentration, adsorbent dose, contact time and temperature. The maximum uptake capacity was 22.1 mg/g at an optimum pH of 4.4. The contact time demonstrates a sharp increase in adsorption capacity at less than 20 min of contact. The equilibrium adsorption process demonstrates that both Freundlich and Langmuir models fit appropriately the sorption model data (R^2 = 0.99 and R^2 = 0.988, respectively). The kinetic process followed a pseudo-second order. The negative value of ΔG is an indication that the activity is feasible and spontaneous. The positive value of ΔH revealed that the adsorption process involves the absorption of heat energy. The positive value of ΔS means that there is increased entropy between the SO dye and the MSF adsorbent.

This study demonstrates that *Senna fistula* (a waste), which is readily available, can be converted to a cost-effective and efficient adsorbent for removing SO from aqueous solutions.

References

[1] M Benjelloun, Y Miyah, G. A Zerrouq, & S. Lairini, "Recent Advances in Adsorption Kinetic Models: Their Application to Dye Types", Arabian Journal of Chemistry **14** (2021) 103031.

[2] S. Mani, P. Chowdhary, & R. N. Bharagava, *Textile Wastewater Dyes: Toxicity Profile and Treatment Approaches*, in: Bharagava, R.N., Chowdhary, P. (Eds.), Emerging and Eco-Friendly Approaches for Waste Management. Springer Singapore, Singapore (2019).

[3] UNESCO WWAP (United Nations World Water Assessment Programme). The United Nations World Water Development Report (2017).

[4] J. B. Tarkwa, N. Oturan, E. Acayanka, S. Laminsi, & M. A. Oturan, "Photo-Fenton oxidation of Orange G azo dye: process optimization and mineralization mechanism", Environmental Chemistry Letters **17** (2019) 473.

[5] M. Sharma, P. Das, S. Dat'ta, *Comparative Study on Adsorption of Dye Solutions Using Silver Nanocomposites* S.K. Ghosh (Ed.), Waste Valorisation and Recycling, Springer Singapore, Singapore (2019).

[6] G.A. Dissanayake L. S. Herath, W. J. Poh, W.J. Ng, "Statistical optimization of glyphosate adsorption by biochar and activated carbon with response surface methodology", Chemosphere **227** (2019) 533.

[7] O. S, Bello, M. A. Moshooda, B. A. Ewetumoa, I. C. Afolabi, "Ibuprofen removal using coconut husk activated Biomass", Chemical Science Transaction **29** (2020) 100533.

[8] C. J. Ajaelu, V. Nwosu, L. Ibironke, A. M. Adeleye, "Adsorptive removal of cationic dye from aqueous solution using chemically modified African Border Tree (Newbouldia laevis) bark", J. Applied Sc. Environ. Mangt. **21** (2017) 1323.

[9] M. S, Sajab, C.H, Chia, S. Zakaria, S. Khiew, "Cationic and anionic modifications of oil palm fruit bunch fibres for the removal of dyes from aqueous solutions", Bioresource Technology **128** (2012) 571.

[10] I. A. W, Tan, B. H. Hameed, "Adsorption isotherms, kinetics, thermodynamics and desorption studies of basic dye on activated carbon derived from oil palm empty fruit bunch", Journal of Applied Science **10** (2010) 2565

[11] M. A. Ahmad, N. Ahmad, O. S. Bello, "Statistical optimization of adsorption process for removal of synthetic dye using watermelon rind", Model Earth System Environment **3** (2017) 1.

[12] O. Uner, U. Gecgel, H. Kolancilar, Y. Bayrak, "Adsorptive removal of Rhodamine blue with activated carbon obtained from Okra wastes", Chemical Engineering Communication **204** (2017) 772.

[13] V. Gedam, P. Raut, A. Chahande, P. D. Pathak, "Kinetic, thermodynamics and equilibrium studies on the removal of Congo red dye using activated teak leaf powder", Applied Water Science **9** (2019) 55.

[14] T. E. Amoo, K. O. Amoo, O. A. Adeeyo, C. L. Ogidi, "Kinetics and equilibrium studies of the adsorption of copper (II) ions from industrial wastewater sing activated carbons derived from sugarcane bagasse", International Journal of Chemical Engineering **2022** (2022) 6928568.

[15] O. S. Bello, A. A. Adegoke, O. O. Sarumi, O. S. Lameed, "Functionalized locust bean pod (Parkia biglobosa) activated carbon for Rhodamine B dye removal", Heliyon **5** (2019) e02323.

[16] A. A. Ikotun, C. A. Olalere, D. O. Adekunle, M. O. Dawodu, "Phytochemistry and antimicrobial studies of African black soap and its modified samples", Journal of Chemical and Pharmaceutical Research **9** (2017) 354.

[17] A. A. Ikotun, O. F. Ogundele, O. M. Kayode, C. J. Ajaelu, "Chemical and biological significance of naturally occurring additives on African black soap and its performance", Journal of Applied Sciences and Environmental Management **21** (2017) 1370.

[18] A. A. Ikotun, M. P. Coogan, A. A. Owoseni, G. O. Egharevba, "Design, synthesis, physicochemical and antimicrobial properties of rhenium (I) tricarbonyl complexes of 3-(phenylimino)indole-2-one", Journal of Chemical Society of Nigeria **44** (2019) 948.

[19] J. C. Ajaelu, J. T, Bamgbose, B. O. Atolaiye, A. A. Adetoye, "The use of cyanomethemoglobin complex in estimating cyanogens potential of cassava and cassava products", African Journal of Biotechnology **7** (2008) 1585.

[20] S. Chakraborty, A. Mukherjee, S. Das, N. R. Maddela, S. Iram, P. Das. 2021, "Study on isotherm, kinetics and thermodynamics of adsorption of crystal violet dye by calcium oxide modified flash ash", Environmental Engineering Research **26** (2021) 190372.

[21] N. U. M. Nizam, M. M. Hanafiah, E. Mahmoudi, A. A. Halim, A. W. Mohammad, "The removal of anionic and cationic dyes from an aqueous solution using biomass-based activated carbon", Scientific Reports 11 (2021) 8623.

[22] S. J. Olusegun, N. D Mohallem, "Comparative adsorption mechanism of doxycycline and congo red using synthesized kaolinite supported CoFe2O4 nanoparticles", Environ. Pollut. **260** (2020) 114019.

[23] Y. Hu, T. Guo, X. Ye, Q. Li, M. Guo, H. Liu, "Dye adsorption by resin: Effect of ionic strength on hydrophobic electrostatic interactions", Chemical Engineering Journal **228** (2013) 392.

[24] E. Mahmoudi, S. Azizkhani, A. W. Mohammad, L. Y. Ng, A. Benamor, W. L. Ang, M. Ba-Abbad, "Simultaneous removal of congo red and cadmium (II) from aqueous solutions using graphene oxide-silica composite as a multifunctional adsorbent", J. Environ. Sci. **98** (2020) 151.

[25] J. Wang, W. Zhang, X. Kang, & C. Zhang, "Rapid efficient recovery of silver with nanoscale zerovalent iron support high-performance activated carbon derived from straw biomass", Environ. Pollut. **255** 113043 (2019).

[26] S Razzaq, M. Akhtar, S. Zulfiqar, S. Zafar, I. Shakir, P. O. Agboola, S. Haider, M. F. Warsi, "Adsorpton removal of Congo red onto L-cysteine/rGO/PANI nanocomposite: equilibrium, kinetics and thermodynamic studies", Journal of Taibah University for Science **15** (2021) 50.

[27] Y.S. Ho, G. McKay, "Pseudo-Second Order Model for Sorption Processes", Process Biochemistry **34** (1999) 451.

[28] I. Melcakova, T. Ruzovic, "Biosorption of zinc from aqueous solution using algae and plant biomass", Nova Biotechnologica **10** (2021) 22.

[29] J. O. Ighalo, A G. Adeniyi, "Adsorption of pollutants by plant bark - derived adsorbents: An empirical review", Journal of Water Process Engineering **35** (2020) 101228.

[30] C. J. Ajaelu, E. O. Faboro, "Adsorption of copper (II) ions onto raw Globimetula oreophila (Afomo ori koko) leaves", African Journal of Biotechnology **20** (2021) 122.

[31] K. O. Sodeinde, S. O. Olusanya, D. U. Momodu, V. F. Enogheghase, O. S. Lawal, "Waste glass: An excellent adsorbent for crystal violet dye, Pb^{2+} and Cd^{2+} heavy metal ions decontamination from wastewater", J. Nig. Soc. Phys. Sci. **3** (2021) 414.

[32] C. J. Ajaelu, L. Ibironke, A. B. Oladinni, "Copper (II) ions adsorption by Untreated and Chemically Modified Tectona grandis (Teak bark): Kinetics, Equilibrium and thermodynamic Studies", African Journal of Biotechnology **18** (2019) 296

[33] C .J. Ajaelu, M. O. Dawodu, E O. Faboro, O. S Ayanda, "Copper Biosorption by Untreated and Citric Acid Modified *Senna fistula* Leaf Biomass in a Batch System: Kinetics, Equilibrium and Thermodynamics Studies", Physical Chemistry **7** (2017) 31.

[34] O. Alao O., C. J. Ajaelu, O Ayeni, "Kinetics, Equilibrium and Thermodynamic Studies of the Adsorption of Zinc on Carica papaya root powder", Research Journal of Chemical Sciences **4** (2014) 1.

[35] O. S. Bello, M. A. Moshooda, B. A. Ewetumoa, I. C. Afolabi, "Ibuprofen removal using coconut husk activated Biomass", Chemical Science Transaction **29** (2020) 100533.

[36] A.F. A. Hussain and M. H. Halboos, "Adsorption of safranin dye from their aqueous solutions by using CA and Nano FeO/CA", J. Phys.: Conf. Ser. **1660** (2020) 012080.

[37] M. R. Malekbala M, S. M. Soltani, S. K. Yazdi, S. Hosseini, "Equilibrium and Kinetic Studies of Safranine Adsorption on Alkali-Treated Mango Seed Integuments", International Journal of Chemical Engineering and Applications **3** (2012) 160.

[38] K. O. Adebowale,B. I, Olu- Owolabi, E. C. Chigbundu, "Removal of Safranin-O from Aqueous Solution by Adsorption onto Kaolinite Clay", Journal of Encapsulation and Adsorption Sciences **4** (2014) 89.

[39] V. Chandane, V.K. Singh, "Adsorption of safranin dye from aqueous solutions using a low-cost agro-waste material soybean hull", Desalination and Water Treatment **57** (2016) 4122.